Designing a Fast-Igniting Catalytic Converter System

Jason M. Keith, Hsueh-Chia Chang, and David T. Leighton, Jr.
Dept. of Chemical Engineering, University of Notre Dame, Notre Dame, IN 46556

Through analysis and numerical simulation, the late lightoff (~ 3 min) of the current automobile catalytic converter is attributed to a downstream ignition phenomenon that is unstable to flow-rate fluctuations. A design is proposed which incorporates a stable and thermally efficient leading-edge ignition. The key feature involves diverting a small portion of exhaust gas through a bypass stream, which contains an electric preheater and a preigniter, during startup. This allows the preheater to utilize a low power input using the existing battery and yet raise the gas temperature beyond a precise minimum that rapidly lights off the entire preigniter. The hot preigniter is then used to light off the main catalytic converter. Removal of the bypass after complete ignition preserves the preigniter catalyst, a major advantage. The optimal design is shown to lightoff within 10 s and reduce pollution by almost 90% over current designs and thus meet ultra low emission vehicle (ULEV) standards.

Introduction

There has been a great deal of research in catalytic converter technology since its inception in the mid 1970s. The first type of converter was developed to oxidize carbon monoxide gas (CO) and hydrocarbons (HC) that formed during incomplete gasoline combustion. However, oxides of nitrogen (NO_x) passed through the converter unreacted. As a result, these first catalytic converters were referred to as oxidation converters or two-way converters (2WC), as they eliminated two of the three major pollutants via oxidation reactions. The active metal in these first 2WCs was primarily platinum, although later converters contained various concentrations of platinum, rhodium, and palladium.

As recently as the Clean Air Act of 1990, federal standards mandated smaller levels for all three pollutants. Research devoted toward developing new catalyst materials capable of the oxidation of CO and HC in addition to reduction of NO_x was put to use in the three-way converter (3WC), which contains mostly palladium. Today's catalysis research efforts focus on finding materials to catalyze pollutant conversion reactions at higher rates and on developing converters that can maintain effective pollution reduction after being aged for over one hundred thousand miles. There are also efforts to develop new catalysts to reduce NO_x pollution beyond the limits of the 3WC.

Another approach is to utilize the current catalyst, but to improve the thermal and other transport properties of the converter based on the principles of reaction engineering. The 3WC is actually very effective in reducing pollution after it has heated up, or ignited. However, pollution is most severe when the exhaust systems begin from what is known as a cold start, when the converter is at ambient temperature and the vehicle has not been started. Such cold-start tests are the most difficult part of the Federal Test Procedure (FTP test), which specifies vehicle speed as a function of elapsed test time, as seen in Figure 1. More detailed FTP data for a specific automobile are available in the article of Oh et al. (1993) and include engine-out mass flow rate, HC concentration, and temperature, as shown in Figure 2. These data clearly indicate that the initial minutes after starting a car when the converter is still cold are crucial in beating the strict pollution limits set forth by the new clean-air laws. Therefore, the focus of converter research today is now geared toward minimizing the duration of this unignited period. As a result, many novel techniques have been developed to accomplish this task, including hydrocarbon traps, preigniters, and electrically heated catalytic converters (Jacoby, 1999).

Correspondence concerning this article should be addressed to J. M. Keith.
Present address of J. M. Keith: Department of Chemical Engineering, Michigan Technological University, Houghton, MI 49931.

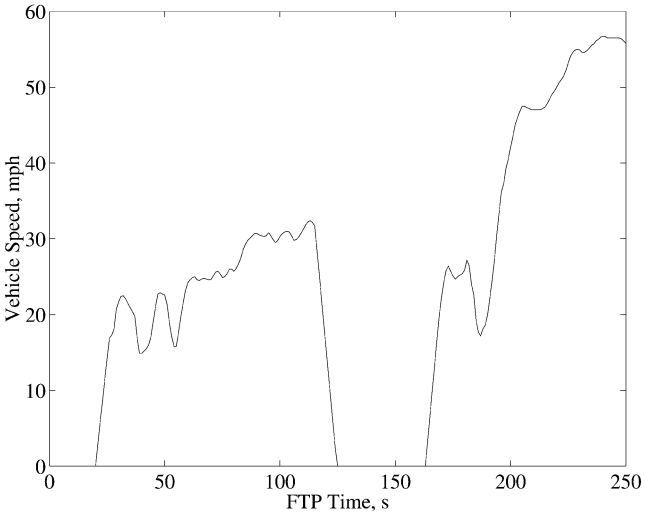

Figure 1. Vehicle speed as a function of elapsed time for the first 250 s of the Urban Dynamometer Driving Schedule portion of the FTP test.

The converter designs and options currently available will be qualitatively and quantitatively evaluated in this article, culminating in a new design of an inexpensive, rapidly igniting catalytic converter system. This evaluation will be facilitated through the extension of an existing analytical theory (Leighton and Chang, 1995) for converter ignition during step-change tests to more realistic driving conditions such as the FTP driving cycle. The modified theory, verified through numerical simulations of a cold start, will be used to design an optimum automobile exhaust system that will work well under all startup conditions.

Model Equations for the Catalytic Converter

The two-way catalytic converter was first simulated by Oh and Cavendish (1982). Their model is presented below, and is used in this article for both numerical and analytical models in order to predict ignition times for various operating and design conditions. This converter, with parameters listed in Table 1, will serve as a model for comparison purposes, and in this manuscript will be referred to as the standard converter. Also, in order to compare key design parameters for this standard converter with other designs, a standard condition is defined. This standard condition uses a temperature of 600 K and the concentrations listed in Table 2, consistent with the step-change conditions of Oh and Cavendish (1982) and Leighton and Chang (1995).

Because of the high solid/gas thermal capacitance ratio, given by

$$\gamma = \frac{(\rho C_p)_s}{(\rho C_p)_g} \frac{(1-\epsilon)}{\epsilon}, \tag{1}$$

where the gas capacitance $(\rho C_p)_g$ is given as 6.3×10^{-4} J/K·cm^3, the gas temperature and concentration equilibrate much more rapidly than the solid temperature. Therefore, the dynamics governing conservation of mass and energy in the gas

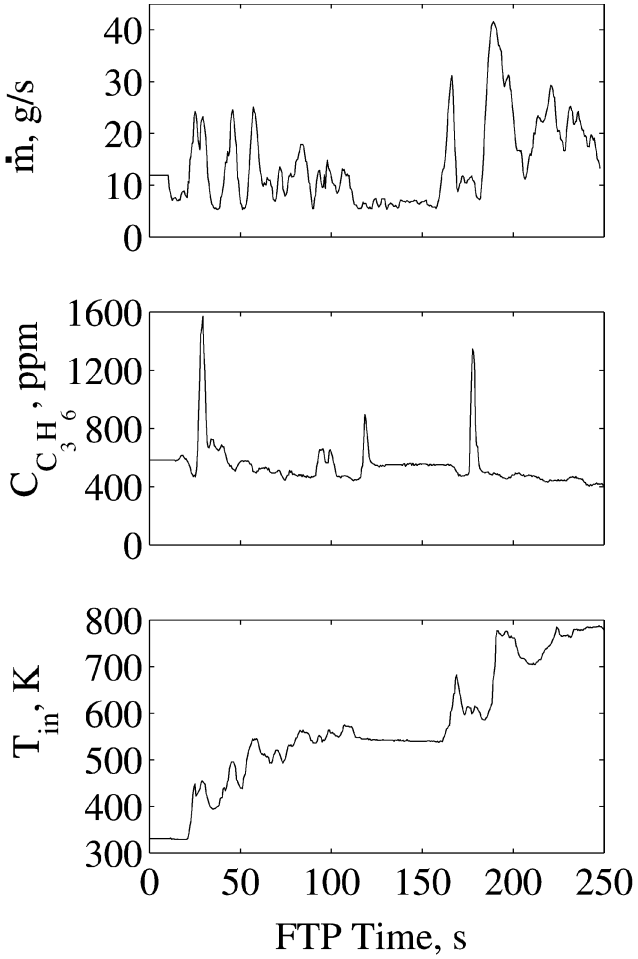

Figure 2. Engine-out mass flow rate, hydrocarbon concentration, and gas temperature for FTP test.

These data, originally used by Oh et al. (1993), are used for numerical and analytical models.

phase are quasi-steady compared with their solid-phase counterparts. Moreover, as shown by Leighton and Chang, transverse spatial variation in the solid phase can be neglected during the long-time thermal dynamics leading to ignition. As such, both phases can be lumped in the transverse direction and the gas phase is at steady state. The gas equations are then

Table 1. Comparison of Reactors

Quantity	Ceramic Monolith	Loaded Preigniter	Heated Preigniter
L (cm)	10.0	2.0	2.54
a (cm)	0.06062	0.06000	0.07700
Δz (cm)	0.0130	0.0047	0.0053
ϵ	0.6836	0.8800	0.8800
$(\rho C_p)_s$ (J/K·cm^3)	2.678	2.678	2.310
κ_s (J/K·s·cm)	0.01675	0.01675	0.01627
h (J/K·s·cm^2)	0.0169	0.0171	0.0133
a_{cat} (cm^2 Pt/cm^3)	269	269	650
S (cm^2/cm^3)	23.09	28.82	22.83
V_H (cm^3)	0.00	0.00	228.35

Table 2. Standard Condition Engine-Out Concentrations

Species	Concentration (Mol Fraction)
CO	0.02
HC (as C_3H_6)	450×10^{-6}
CH_4	50×10^{-6}
H_2	0.0067
O_2	0.05
NO_x (as NO)	500×10^{-6}

Note: Feed temperature 600 K; initial temperature 300 K.

$$\epsilon U\frac{\partial C_{g,i}}{\partial x} = -k_{m,i}S\left(C_{g,i}-C_{s,i}\right) \tag{2}$$

and

$$\epsilon\left(\rho C_p\right)_g U\frac{\partial T_g}{\partial x} = hS\left(T_s-T_g\right). \tag{3}$$

A converter operating with the standard mass flow rate of 40 g/s has a corresponding gas-phase channel velocity U of 1,680 cm/s. The conservation of mass and energy equations for the solid phase are

$$a_{\text{cat}}R_i(C_s,T_s) = \frac{\rho_g}{M_g}k_{m,i}S\left(C_{g,i}-C_{s,i}\right) \tag{4}$$

and

$$(1-\epsilon)\left(\rho C_p\right)_s\frac{\partial T_s}{\partial t} = \kappa_s(1-\epsilon)\frac{\partial^2 T_s}{\partial x^2} + hS\left(T_g-T_s\right) + a_{\text{cat}}\sum_{i=1}^{4}(-\Delta H)_i R_i(C_s,T_s) + \frac{P}{V_H}, \tag{5}$$

where P/V_H is the electric power input per unit volume of the monolith. When there is no electrical heating, this term can be set equal to zero. Variation in temperature from one channel to the next due to flow nonuniformity and radiation effects are neglected because they do not contribute significantly to converter ignition (Chen et al., 1988; Oh and Bissett, 1994). Therefore a simple one-dimensional, one-channel model is employed here for analytical and numerical simplicity.

In Eqs. 4 and 5 the parameter a_{cat} represents the catalyst loading. Data are available in the literature with regard to noble metal loading levels (Chen et al., 1988). For a typical in-use, aged two-way oxidation catalyst, the loading a_{cat} is 269 cm^2 Pt/cm^3 reactor, roughly 15% of the fresh loading level of 1,793 cm^2/cm^3. The catalyst loading decreases as a function of vehicle age because of sintering at high catalyst temperatures (when active sites fuse together, rendering some useless) and because of posioning (by poisons present in the exhaust). The upper limit for the noble-metal loading for highly loaded converters is taken to be 2500 cm^2 Pt/cm^3. Depending on the state of the catalytic converter being studied, these values will be used in this article for the noble-metal loading a_{cat}.

For the standard converter, the reaction rates from Eqs. 4 and 5 have been determined as the following (Oh and Cavendish, 1982):

$$R_{\text{CO}} = k_1 C_{\text{CO}} C_{\text{O}_2}/G \tag{6}$$

$$R_{\text{C}_3\text{H}_6} = k_2 C_{\text{C}_3\text{H}_6} C_{\text{O}_2}/G \tag{7}$$

$$R_{\text{CH}_4} = k_3 C_{\text{CH}_4} C_{\text{O}_2}/G \tag{8}$$

$$R_{\text{H}_2} = k_1 C_{\text{H}_2} C_{\text{O}_2}/G \tag{9}$$

and

$$R_{\text{O}_2} = 0.5R_{\text{CO}} + 4.5R_{\text{C}_3\text{H}_6} + 2R_{\text{CH}_4} + 0.5R_{\text{H}_2}, \tag{10}$$

where

$$G = T\left(1+K_1C_{\text{CO}}+K_2C_{\text{C}_3\text{H}_6}\right)^2\left(1+K_3C_{\text{CO}}^2C_{\text{C}_3\text{H}_6}^2\right)\times\left(1+K_4C_{\text{NO}}^{0.7}\right), \tag{11}$$

indicating that CO and HC oxidation are self-inhibiting. The rate constants are given as the following (Oh and Cavendish, 1982):

$$k_1 = 6.699\times10^9\exp(-12{,}556/T_s) \tag{12}$$

$$k_2 = 1.392\times10^{11}\exp(-14{,}556/T_s) \tag{13}$$

$$k_3 = 7.326\times10^6\exp(-19{,}000/T_s) \tag{14}$$

and

$$K_1 = 65.5\exp(961/T_s) \tag{15}$$

$$K_2 = 2.08\times10^3\exp(361/T_s) \tag{16}$$

$$K_3 = 3.98\exp(11{,}611/T_s) \tag{17}$$

$$K_4 = 4.79\times10^5\exp(-3{,}733/T_s). \tag{18}$$

It is noted that the following analytical ignition model will be valid for any kinetic rate laws. The kinetics presented here are meant to serve only as an illustrative example.

The engine-out data from the cold-start portion of the Federal Test Procedure (FTP test) from Figure 2 will be used as a boundary condition for gas temperature and concentration at the converter inlet at $x = 0$, where engine-out concentrations are assumed to be proportional to the HC concentration. This data set will serve as an appropriate test case to scrutinize the analytical ignition model to be developed in the next section with direct numerical simulations. Despite the fact that the engine-out temperature in modern vehicles may be higher due to a close-coupled converter design and that the individual species concentrations may independently fluctuate in different ratios, these assumptions will be used for the ensuing analysis, as the predictive model to be developed in the next section will be valid for any temperature and pollutant concentration history.

Transient fluctuations in the mass flow rate through the system will also be varied through the channel velocity U dur-

ing these simulations. Equations 2–5 will be numerically integrated to yield temperature and species concentration profiles in both the gas and solid phases of the converter as a function of time. During a typical ignition simulation, the exit pollutant concentration will decrease only slightly, as there is negligible conversion. However, a point in time will be reached when the exit gas CO concentration at $x = L$ rapidly drops to near zero. This time is defined as the ignition time, which will be numerically estimated for various converter designs.

Analytical Ignition Model for Transient Feed Conditions

Consider the performance of an automobile catalytic converter subjected to a step change in inlet temperature. A theory has been developed by Leighton and Chang (1995) that predicts the resulting delay time before converter ignition, t_{ig}. There are two key parameters in this theoretical model. The first parameter, χ, quantifies the strength of longitudinal thermal dispersion in a catalytic converter, as it measures the square of the dispersion length ($\sqrt{\alpha_{\text{eff}} t_{\text{ig}}^{\infty}}$) to convection length ($U_{\text{eff}} t_{\text{ig}}^{\infty}$) ratio during the characteristic ignition time t_{ig}^{∞}:

$$\chi = \frac{\alpha_{\text{eff}}}{U_{\text{eff}}^2 t_{\text{ig}}^{\infty}}, \tag{19}$$

where $U_{\text{eff}} = U/\gamma$ is the effective thermal velocity in the converter and α_{eff} is the effective Taylor-Aris axial thermal dispersivity (Taylor, 1953; Aris, 1956; Leighton and Chang,1995; Keith et al., 1999) induced by transverse temperature differences between the gas and solid phases. Derived through asymptotic expansion, it is a function of the gas velocity, U, monolith pore radius a, capacitance ratio, γ, and the gas thermal diffusivity, $\alpha_g = 0.746$ cm^2/s:

$$\alpha_{\text{eff}} = \frac{11}{48} \frac{U^2 a^2}{\alpha_g \gamma}. \tag{20}$$

The second key parameter of Leighton and Chang's model is the homogeneous ignition time, t_{ig}^{∞}, the time at which the reactor will ignite in the hypothetical limit of equal gas and solid temperatures in the catalytic converter:

$$t_{\text{ig}}^{\infty} = \frac{(1-\epsilon)(\rho C_p)_s}{A\beta}. \tag{21}$$

In the previous equation, A and β arise from a zeroth-order kinetics approximation to the reaction rates in Eq. 5, which is valid for small values of β^{-1} when the reaction is a very rapid process:

$$a_{\text{cat}} \sum_{i=1}^{4} (-\Delta H)_i R_i(C_s, T_s) \sim A \exp\left[\beta\left(T_s - T_g^{\text{in}}\right)\right]. \tag{22}$$

Under these conditions, reactant consumption can be ignored during the ignition process and only the thermal equations (Eqs. 3 and 5) need to be considered to predict the step-change ignition time, t_{ig}. The assumption of small β^{-1} should also hold for other rate expressions characteristic of catalytic converter ignition (in addition to the ones used here). Graphs of the product $A\beta$, homogeneous ignition time, t_{ig}^{∞}, computed ignition time, t_{ig}, and dispersion parameter, χ, are shown in Figures 3a–3c as a function of feed temperature, T_{in}, for the standard converter studied by Oh and Cavendish (1982) and Leighton and Chang (1995).

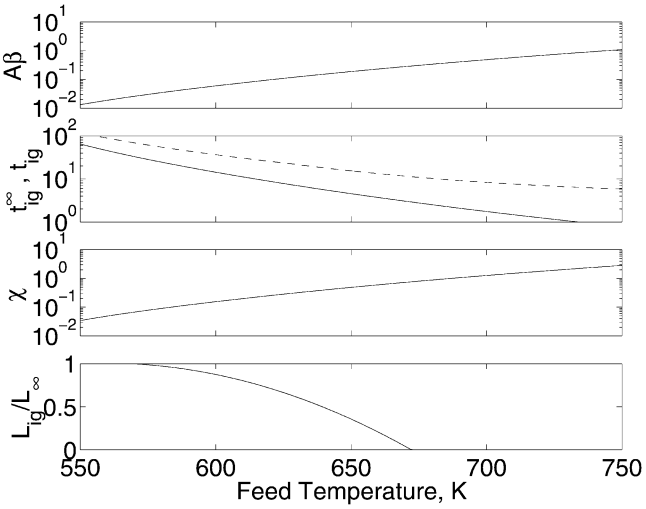

Figure 3. Parameters $A\beta$, homogeneous and computed ignition times [t_{ig}^{∞} (solid line) and t_{ig} (dashed line)], dispersion parameter, χ, and dimensionless ignition length, L_{ig}/L_{∞} (as predicted by Leighton and Chang), as a function of feed temperature, T_{in}, for the standard converter of Oh and Cavendish.

In the limit $T_s = T_g$ there is no thermal dispersion, and thus $\chi = 0$ and $t_{\text{ig}} = t_{\text{ig}}^{\infty}$. Furthermore, the axial location of the downstream ignition is given by the homogeneous ignition length, $L_{\infty} = U_{\text{eff}} t_{\text{ig}}^{\infty}$. Although designed to maximize interphase heat transfer, gas and solid temperatures differ slightly in real catalytic converters. This noninfinite interphase heat transfer induces a transient Taylor-Aris thermal dispersivity, α_{eff}, over the time it takes for the two phases to reach thermal equilibrium, such that $\chi > 0$. This dispersion smooths the sharp front at the step such that ignition is now delayed and occurs at a time $t_{\text{ig}} > t_{\text{ig}}^{\infty}$, but at a shorter length $L_{\text{ig}} < L_{\infty}$. These effects are illustrated in Figures 3b and 3d.

Leighton and Chang's analytical model predicts step-change ignition times, t_{ig}, under these circumstances in two asymptotic limits. Under the standard conditions used in Oh and Cavendish (1982) and during the city driving phase of the FTP test, the ignition time is much greater than the time required for the gas and solid phases of the standard converter to reach thermal equilibrium. As a result, the gas- and solid-phase temperatures are roughly equal during the time it takes for the converter to ignite, and $\chi \ll 1$, as there is little thermal dispersion. A thermal front will remain sharp as it travels down the monolith and ignition will occur at this front

near the exit of the converter, at a time

$$\frac{t_{ig}}{t_{ig}^{\infty}} = 1 + 2\chi^{1/2}\left|\ln\left(\frac{\chi^{1/2}}{2\eta}\right)\right|^{1/2} \tag{23}$$

and length $L_{ig} \sim L_{\infty}$. In Eq. 23, η measures the monolith subcooling, given by $\eta = \beta(T_g^{in} - T_s^0)$. Because of the ignition location, the physical ignition process under "small χ conditions" is referred to as a downstream ignition.

Increasing the engine-out gas temperature of the standard condition from 600 K to 700 K dramatically changes the ignition behavior. Such a high engine-out gas temperature will physically occur during the highway driving phase of the FTP test. Under these new, nonstandard conditions, the homogeneous ignition time, t_{ig}^{∞}, is reduced (as seen in Figure 3d) because of the larger reaction rate, which also essentially reduces the strength of interphase heat transfer in the converter. The large Taylor-Aris thermal dispersion that arises ($\chi \sim 1$) smooths a thermal front as it enters the bed, such that the converter will ignite at the entrance, far upstream of the homogeneous ignition length, L_{∞}. Because of the ignition location, the physical ignition process under "large χ conditions" is referred to as a leading-edge ignition. The ignition time is significantly greater than the homogeneous ignition time t_{ig}^{∞} and is given by:

$$\frac{t_{ig}}{t_{ig}^{\infty}} = 2.50 + \chi(\ln\eta - 0.34). \tag{24}$$

As may be seen from Figure 3b, however, t_{ig} is still a strongly decreasing function of temperature.

The location of both downstream and upstream ignition is given by:

$$L_{ig} = U_{eff} t_{ig}^{\infty} f(\chi), \tag{25}$$

where $f(\chi)$ is derived by Leighton and Chang, and is reproduced in Figure 3d. The limit $f(\chi) = 1$ is reached when χ approaches zero (such as the gas and solid phase temperatures are equal) when the step-change ignition occurs at the homogeneous ignition length L_{∞}. Furthermore, $f(\chi)$ will decrease monotonically as the strength of the dispersion χ increases such that $f(\chi) = L_{ig} = 0$, when χ is of order unity or greater. For the current converter, this transition occurs when the inlet gas temperature T_{in} exceeds 675 K.

Provided that the ignition length L_{ig} is less than the converter length L, the step-change ignition will occur within the reactor at time t_{ig}. If L_{ig} is greater than L, the converter will never ignite. If $L_{ig}/L \sim 1$, a downstream ignition occurs, while for $L_{ig}/L \ll 1$, an upstream leading-edge ignition occurs. Leighton and Chang (1995) have delineated a crucial advantage of leading-edge ignition: the heat released during this ignition is readily convected downstream to light off the entire converter in just a few additional seconds. This heat is wasted in a downstream ignition, and the entire converter can be ignited only by the slow process of upstream thermal heat diffusion, which can take several minutes.

There is another major advantage to redesigning the converter to ignite under the large χ leading-edge ignition mechanism. Fluctuations in flow rate will have a strong effect on the ignition location when χ is small. These fluctuations may convect the step-change ignition location to a point outside of the reactor. In this instance, ignition will not take place and pollution levels may be very high as a result. However, fluctuations in flow rate have a very small impact at large dispersion levels, when χ is of order unity or greater. The ignition will occur at or near the leading edge of the converter, regardless of the flow rate. There is hence every reason to increase T_{in} beyond 700 K to allow χ to exceed unity. The impact of fluctuations on ignition is studied in more detail in a later section.

Equations 19–25, derived by Leighton and Chang, assume that the temperature and concentration feed to the converter are constant during a specific step-change experiment or simulation. However, a catalytic converter subject to the FTP test has a fluctuating temperature, concentration, and flow rate. Despite this fact, the theory of Leighton and Chang will be extended and shown to be valid for leading-edge ignition in the presence of flow fluctuations, as in the FTP test, and will hence be used to design an optimized, rapidly igniting catalytic converter system.

The analysis begins by breaking up the FTP temperature and concentration data into a discrete series of many small step changes (time interval = 1 s) as a function of the FTP elapsed time, t_{FTP}. Assuming that the engine-out temperature and pollutant concentration remain constant, a separate step change ignition time, t_{ig}, will be computed for every step change from Eq. 23 or 24 (depending on the value of χ). The total elapsed FTP time required for the converter to ignite subject to a particular step change is the sum of the elapsed time prior to the introduction of the step change plus the step change ignition time, $t_{FTP} + t_{ig}$. The minimum of this quantity will be the FTP ignition time, provided that the computed ignition location is inside the monolith, namely, $L_{ig}/L < 1$. Due to large fluctuations in temperature, concentration, and mass flow rate, there may be large errors in the estimate of the FTP ignition length. Therefore, correction factors for the effective velocity, U_{eff}, homogeneous ignition time, t_{ig}^{∞}, and ignition location, $f(\chi)$, will be derived below that will yield a more reasonable estimate.

The first correction to Eq. 25 is for the effective velocity, U_{eff}. If the velocity were the only parameter to fluctuate, the ignition time, t_{ig}, will be unchanged for any step-change test. This is because Eqs. 23 and 24 are independent of the gas velocity, U. However, the ignition length, L_{ig}, will depend on the velocity, as given by Eq. 25. The location of the ignition will have a significant impact on the FTP ignition time, as a rapid acceleration may lead to an ignition that would take place far beyond the converter length, L. Therefore, a very good estimate for the effective velocity is the mean velocity over the interval from t_{FTP} when the step is introduced to $t_{FTP} + t_{ig}$ when Eq. 23 or 24 predict when ignition will occur:

$$\overline{U_{eff}} = \frac{\int_{t_{FTP}}^{t_{FTP}+t_{ig}} U_{eff}\,dt}{t_{ig}}. \tag{26}$$

The second correction to Eq. 25 is for the homogeneous ignition time, t_{ig}^{∞}. An intense pertubation in temperature and

concentration in the FTP test may predict converter ignition through a small L_{ig}. However, the duration of this pertubation must be equal to the ignition time, t_{ig}, in order to yield an ignition. Therefore, a more accurate estimate of the ignition length, L_{ig}, during transient driving schedules such as the FTP test should not use the instantaneous value of t_{ig}^{∞}, but rather the upper bound of t_{ig}^{∞} over the time interval from t_{FTP} to $t_{FTP} + t_{ig}$ when ignition will occur:

$$\overline{t_{ig}^{\infty}} = \max t_{ig}^{\infty}(t_{FTP}, t_{FTP} + t_{ig}). \tag{27}$$

This correction was found to yield increased but more reasonable prediction of the ignition time t_{ig}, and ignition length, L_{ig}, when compared with numerical simulations.

A third and final correction to Eq. 25 can be made for the function $f(\chi)$. Although $f(\chi)$ varies from 0 to 1, there is little fluctuation over the typical range of χ for the auto specific FTP data of Oh et al. (1993), which is in the range of $0.0 < \chi < 0.1$. Therefore, small corrections to $f(\chi)$ have little effect on the overall prediction and are neglected, and thus $\overline{f(\chi)} = f(\chi)$.

The corrections just detailed can be combined to yield a reasonable, upper bound prediction of the ignition length:

$$\frac{L_{ig}}{L} = \frac{\overline{U_{eff}}\,\overline{t_{ig}^{\infty}}}{L} f(\chi). \tag{28}$$

The converter ignition time can thus be determined in the following manner. First, a plot of L_{ig}/L as a function of time t_{FTP} is constructed. All values of t_{FTP} at which $L_{ig}/L < 1$ indicate the introduction of a step change in temperature and concentration t_{FTP} at which an ignition can occur. Possible FTP ignition times are therefore equal to the sum of the current FTP times t_{FTP} plus the predicted ignition time $t_{ig}(t_{FTP})$:

$$t_{ig}^{FTP} = t_{FTP} + t_{ig}(t_{FTP}), \tag{29}$$

and the actual ignition will occur at the minimum of these times t_{ig}^{FTP}. Therefore, given the concentration, flow rate, and temperature of the gases entering the converter, this theory yields a prediction of the ignition time without recourse to numerical simulation. An example of this theoretical model applied to the standard catalytic converter is shown in the next section.

Performance of Standard Catalytic Converters and Stability of Leading-Edge Ignition

The step-change simulation experiments of Oh and Cavendish (1982) were duplicated by integrating Eqs. 2–18, where model parameters for the gas and solid phases are taken from Tables 1 and 2. The model reproduced for this study agrees well with their simulation of a more complex model. Under the standard conditions, the standard catalytic converter ignites downstream in a time of about 40 s. Meanwhile, raising the engine-out gas temperature to 700 K yields a leading-edge ignition in about 7 s. These model results agree well with the predicted ignition times of the theoretical model of Leighton and Chang (1995). For comparison of the standard converter with other converter designs, the key parameters of Leighton and Chang's model are given here for the standard condition, $t_{ig}^{\infty} = 13.4$ s and $\chi = 0.17$.

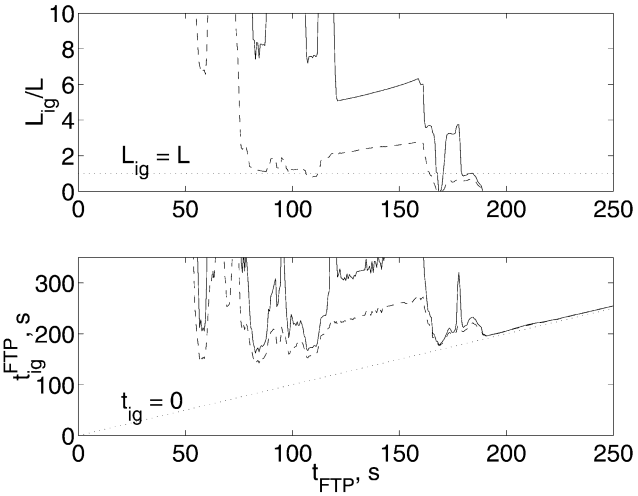

Figure 4. Theoretically computed ignition lengths, L_{ig}, and ignition times, t_{ig}, for the standard converter with (dashed line) and without (solid line) a hydrocarbon trap.

The advantage of the trap is clearly seen, as ignition lengths and times are dramatically reduced with the trap present.

The main focus of the numerical and theoretical models developed in the previous sections were to predict the ignition time using the FTP data as boundary conditions in a transient model. Such a numerical model was developed by Oh et al. (1993) for an electrically heated metal monolith by integrating the model equations of Oh and Cavendish (1982). A similar numerical model will be studied here for various types of converters. The FTP simulations assume CO, NO, H_2, and O_2 are in proportion with the time-dependent HC concentration shown in Figure 2 using the concentrations given in Table 2 as a reference point.

Using these data, the ignition theory derived in the previous section predicts a standard converter lightoff time of 178 s. This is illustrated in the solid line of Figure 4, which shows ignition lengths, L_{ig}, and times, t_{ig}, as a function of elapsed FTP test time, t_{FTP}. The first occurrence at which $L_{ig}/L < 1$ is at about 170 s, as seen in Figure 4a. The ignition time, t_{ig}^{FTP}, can then be read off of Figure 4b. When $t_{FTP} = 170$ s, the ignition time t_{ig}^{FTP} is 178 s. Simulation results provide verification of the theory, as ignition occurs at the leading edge of the converter in a time of 180 s. The ignition is marked by a rapid rise in the maximum solid-phase temperature in the converter T_s as a function of FTP time, as seen in Figure 5.

The FTP driving cycle of Figure 1 can be broken up into two main segments that represent city and highway driving. With the exception of beginning and idling transients, a test vehicle undergoes city driving at a mean speed of about 25 mph during the first 160 s of the FTP driving cycle. Beyond this time, the test vehicle is accelerated at a rapid rate and then driven under highway conditions at a mean speed of 50 mph. During testing, automobiles are driven according to this schedule, and pollution emissions are measured. Study of

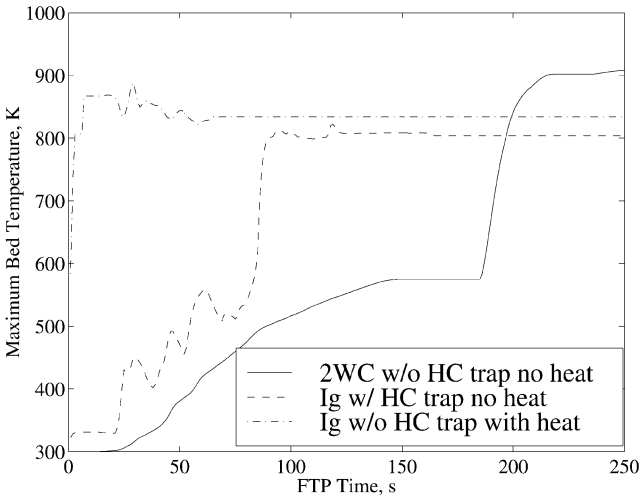

Figure 5. Maximum bed temperature for the standard two-way converter without a hydrocarbon trap and without electric heat (solid line), a highly-loaded preigniter under near-optimum conditions with a hydrocarbon trap and without electric heat (dashed line), and a preigniter with the proposed bypass valve and electric heat without the optional hydrocarbon trap (dash-dot line) as computed by a numerical simulation of the FTP test.

Figure 4 shows that FTP ignition does not occur until the vehicle accelerates to highway speeds because the ignition length $L_{ig}/L \sim 1$ or greater during city driving. Consequently, the stability of the ignition of the standard converter to flow-rate fluctuations must be considered, as under city driving conditions typical of this FTP test, the standard converter may never ignite! If this is the case, extended city driving of a vehicle equipped with such a converter will lead to large pollution levels. This is especially true for aged or poorly maintained vehicles where the catalyst loading can be quite low as a direct consequence of poisoning or sintering. This effectively reduces the value of χ such that leading-edge ignition may not occur even during highway driving.

Figure 6 demonstrates a numerical simulation of a step-change test, which plots axial solid temperature profiles in the standard converter as a function of time. This simulation assumes a constant feed temperature of 590 K, and the pollutant levels given in Table 2, such that $\chi = 0.12$. The mass flow rate through the converter is 15 g/s for the first 40 s of the simulation, corresponding to the flow rate in the FTP test during city driving conditions of about 30 mph. For the duration of the simulation, the mass flow rate is increased to 40 g/s, a typical flow rate during highway driving conditions near 50 mph. It can be seen that an increase in flow rate convects a warm pulse of energy, which is about to ignite, out of the standard catalytic converter, and extinguishes it. This converter will not ignite unless the flow rate drops back down to a level near 15 g/s. Meanwhile, if the flow rate had remained at 15 g/s for the entire simulation, the converter would have ignited in about 50 s. As the average highway journey is several minutes, one might expect very high pollution levels for the entire trip. In reality, the engine-out temperature is expected to increase during a heavy acceleration, leading to converter ignition. However, this example does show the dangers involved in low χ, downstream ignition. Operation of catalytic converters in the large χ, leading-edge ignition limit does not suffer from such drawbacks. Fluctuations in flow rate will not affect ignition at these high dispersion levels.

The impact of such flow-rate fluctuations have been studied in more detail through a series of step change in temperature simulations. In this study, the pollutant concentration fed to the converter is independent of time and is that listed in Table 2. In each simulation the initial temperature of the converter was 300 K and the inlet gas temperature was raised to a fixed value ranging from 550 K to 750 K. These temperatures led to values of χ from 0.034 to 2.8. The time-dependent flow rates used were chosen to mimic various forms of city driving. The periodic mass flow rates were constructed with a mean of either $M = 5.5$, 10.9 (mean flow rate for the FTP test), or 21.8 g/s, and with a minimum flow rate of 5.3 g/s (corresponding to the lowest flow rate observed during idling in the FTP test). The flow rate thus varied over the ranges [5.3, 5.7], [5.3, 16.5], and [5.3, 38.1] g/s, respectively. The period of oscillation τ was chosen to be $\tau = 18.2$ (mean period for the FTP test), 36.4, 72.7 or 145.4 s.

Figure 7 shows a plot of the scaled ignition time t_{ig}/t_{ig}^{∞} as a function of χ for various fluctuation periods τ and mean flow rates M. As claimed earlier, the ignition is stable and insensitive to fluctuations in flow rate at high dispersion levels, corresponding to high engine-out temperatures, and is well-described by the modified step-ignition theory of Leighton and Chang (1995). It can be seen, however, that the converter will not ignite in a length $L_{ig} < L$ if χ is below a critical value. For the standard converter, this level is about 0.05, which corresponds to a critical feed temperature of around 560 K. In fact, the vertical line in Figure 7 corresponds to the minimum idling temperature asymptote at which ignition will occur, 555 K. This lack of ignition is an extremely serious problem for the standard catalytic converter, especially because the engine-out temperature during city driving is less than 550 K, as seen in Figure 2.

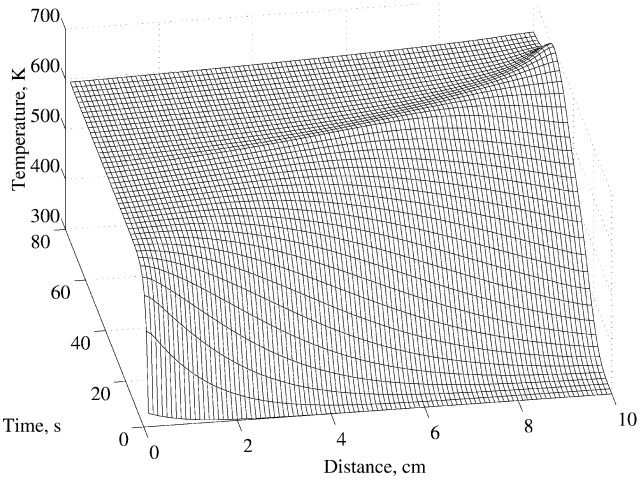

Figure 6. Temperature profiles exhibiting blowout of warm zone under small χ conditions.

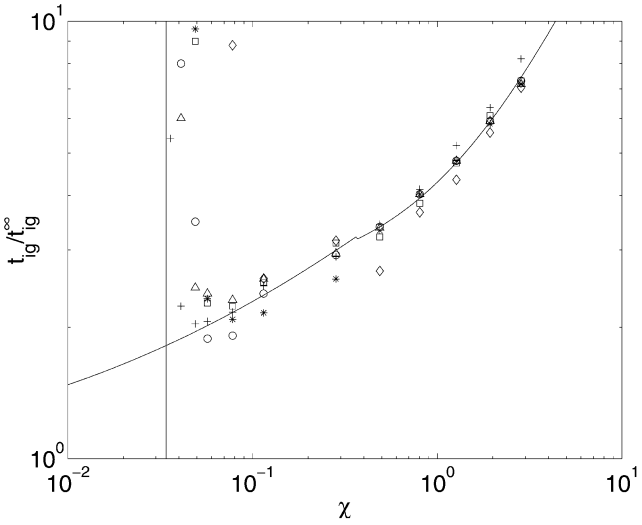

Figure 7. Theoretically computed ignition time (solid line) vs. numerical simulations (symbols) with varying mean flow rate *M* and fluctuation period τ.

The squares correspond to $\tau = 18.2$ s and $M = 10.9$ g/s, the asterisks correspond to $\tau = 36.4$ s and $M = 10.9$ g/s, the circles correspond to $\tau = 72.7$ g/s and $M = 10.9$ g/s, the triangles correspond to $\tau = 145.4$ s and $M = 10.9$ g/s, the diamonds correspond to $\tau = 18.2$ s and $M = 21.8$ g/s, and the plus symbols correspond to $M = 5.3$ g/s with no fluctuation. The vertical line in the figure corresponds to the minimum idling temperature asymptote at which ignition will occur.

This figure also reveals the impact of changes in the mean mass flow rate and fluctuation period on the ignition process. It can be seen that the critical dispersion level χ (and hence critical feed temperature) at which a converter will ignite increases with increasing mass flow rate M and with decreasing fluctuation period τ. This is because the ignition length L_{ig} is proportional to the mass flow rate. With a constant feed temperature, a converter is more apt to ignite if the mean mass flow rate is low or if the fluctuation period is sufficiently large such that a converter can ignite in one half period or less (that is, when the flow rate is always less than the mean). Further evidence of this fact can be seen in Figure 8, which shows the relative CO exit concentration as a function of time for a mean flow rate of $M = 10.9$ g/s and with varying fluctuation periods τ. It is easy to see that at high fluctuation periods the converter ignites, but as the fluctuation period is decreased, the exit concentration actually oscillates, indicating that a potential ignition is extinguished with each period.

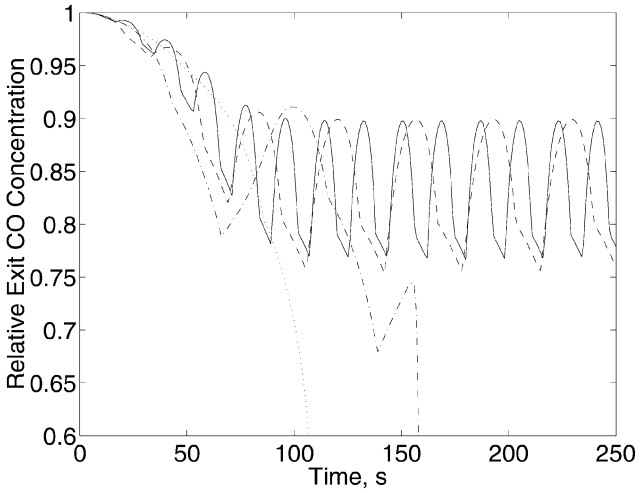

Figure 8. Simulation showing lack of ignition at low fluctuation periods τ.

The solid line corresponds to $\tau = 18.2$ s, the dashed line corresponds to $\tau = 36.4$ s, the dash-dot line corresponds to $\tau = 72.7$ s, and the dotted line corresponds to $\tau = 145.4$ s. The engine-out concentration drops to zero for high fluctuation periods, but oscillates for low fluctuation periods.

These results explain why the standard converter does not ignite during the city driving cycle of the FTP test. Since a large majority of driving trips are spent in city driving, getting to a major highway, or stuck in a traffic jam on one, this lack of ignition during real driving conditions may be a reason why pollution levels continue to increase dramatically, despite the improvements in catalytic converter technology. This underscores the need for a converter capable of stable ignition during city driving when engine-out temperatures are low.

Redesign of Automobile Exhaust Systems

Because of the relatively poor performance of the standard converter during the FTP test, there has been a shift in focus toward novel techniques to improve converter performance. These techniques include hydrocarbon traps (Burk et al., 1995; Lafyatis et al., 1998), highly loaded and low thermal capacitance preigniters (Leighton and Chang, 1995; Roychoudhurry et al., 1997), and electrically heated monoliths (Oh et al., 1993; Oh and Bissett, 1994; Kirchner and Eigenberger, 1996). Each of these novel units will now be studied in detail using the modified analytical ignition theory, verified with numerical simulations. It will be shown that the performance of these novel catalytic converter systems suffer from the same problem of extinction during flow-rate fluctuations.

Hydrocarbon trap

Hydrocarbon traps (HC traps) were developed to significantly reduce hydrocarbon emission from automobile exhausts. At low engine-out temperatures, hydrocarbons adsorb to a zeolite material coated on the surface of a honeycomb monolith. At higher engine-out temperatures, hydrocarbons desorb from the zeolite surface and exit the HC trap. If the hydrocarbons desorb after the downstream main converter (similar to the standard converter outlined earlier) ignites by CO oxidation, they can be combusted in the main converter. Using such a technique, hydrocarbon pollution can be reduced to meet current standards.

In addition to providing less pollution to the environment, HC traps provide other advantages to catalytic converter systems. Examination of the G term in Eqs. 6–10 indicates that the rate of combustion increases with decreasing CO and C_3H_6 concentrations in many regions due to the underlying self-inhibiting competitive Langmuir-Hinshelwood kinetics. Therefore, if an efficient hydrocarbon trap were to reduce the concentration of C_3H_6 to zero, the reaction rate of CO could be increased, which would reduce the homogeneous

ignition time, t_{ig}^{∞}, while also raising the level of χ. Consequently, the addition of a hydrocarbon trap might improve the stability of the catalytic converter ignition to large fluctuations in flow rate.

For the standard converter of Oh and Cavendish (1982), subject to the standard condition shown in Table 2, removing the HC lowers t_{ig}^{∞} to 9.7 s and raises χ to 0.24. Results of the analytical ignition model are summarized in the dashed line of Figure 4, which predicts that the presence of the HC trap reduces the downstream ignition length L_{ig} such that ignition of the converter can occur under city driving conditions in 148 s. Numerical simulations verify this result, predicting ignition in 155 s, a modest reduction. This result is especially important during real, non-FTP, extended city driving conditions, and may indicate that the HC trap is a good start in solving the cold-start problem. The trap alone is not enough, however, to meet LEV or ULEV standards because the large ignition time only reduces CO pollution by about 15%.

Hydrocarbon traps have several drawbacks that may prevent ignition during city driving. If the trap does not adsorb all of the hydrocarbons in the engine exhaust, L_{ig} may be increased beyond the converter length, preventing ignition. This can happen in two circumstances. The first involves the affinity of HC traps to preferentially adsorb water molecules over hydrocarbons (Lafyatis et al., 1998; Jacoby, 1999). The second, and most important circumstance lies in the inability of the HC trap to hold stored hydrocarbons long enough (Jacoby, 1999). HC desorption can occur at temperatures as low as 600 K, before the main converter can ignite.

Even if a HC trap were developed to store all of the exhaust hydrocarbons until a higher temperature, the main converter still ignites at its exit. A small increase in the mass flow rate can push the ignition location beyond the converter exit, preventing ignition from taking place. As a result of these concerns, it remains necessary to find a design that yields a stable and more rapid ignition to avoid high hydrocarbon emissions, even in the presence of such hydrocarbon traps.

Preigniter

Preigniters are miniature converters placed upstream of the main converter, designed to ignite rapidly so that the hot gases leaving the preigniter will quickly heat up and ignite the leading edge of the main (standard) converter. Most preigniters generally contain thinner monolith walls, and thus have a higher void fraction ϵ. Some preigniters also contain higher degrees of catalyst loading, a_{cat}, which increases the reaction rate through the parameter A. Both of these design modifications reduce the homogenous ignition time, t_{ig}^{∞}, while raising the value of χ, both advantages in the cold-start problem. The preigniter therefore plays a key role in reducing emissions, but it must be short and lightly loaded with catalyst to reduce cost; one does not want a second converter, as is often the case for current preconverters. For example, a 2-cm igniter with $a_{cat} = 807$ cm^2 Pt/cm^3, three times the standard loading, requires an additional 60% of precious metal catalyst beyond that of the standard converter. The ultimate design will ignite robustly via the leading-edge mechanism, yet with the standard loading of oxidation catalyst.

One such preigniter was proposed for use by Leighton and Chang to dramatically reduce the ignition time during a specific step-change test (1995). This preigniter will be reexamined here by focusing on the amount of catalyst loading required, taking into account catalyst aging. Although realistic noble-metal loadings are 269 cm^2 Pt/cm^3 for aged (as on the standard catalytic converter) and 1,793 cm^2 Pt/cm^3 for fresh catalyst, the loading will be varied here to determine its effect on converter performance and pollution reduction. Other parameters of this light, highly loaded two-way preigniter are given in Table 1. Under the standard condition of Table 2, this preigniter (with $a_{cat} = 807$ cm^2 Pt/cm^3) has a homogeneous ignition time, $t_{ig}^{\infty} = 1.9$ s and a χ value of 0.38, which is below the $\chi = 1$ design objective. The analytic ignition model, summarized in Figure 9, shows plots of the ignition length L_{ig}/L and the ignition time, t_{ig}, for preigniters without hydrocarbon traps, and agrees well with FTP simulations. Significant pollution reduction occurs with a catalyst loading of five times more than that of the standard converter, when ignition times are reduced to under 2 min. The maximum temperature of such a preconverter as a function of FTP time is shown in Figure 5. However, the catalyst loading is expected to decrease as the vehicle ages, leading to an increase in the ignition length and the possibility of extinction after 50,000 to 100,000 mi. It is hence unlikely that an inexpensive preigniter can be constructed to meet the design objective for the lifetime of the automobile.

This example illustrates that the incorporation of a preigniter into an exhaust system suffers from a serious drawback: downstream or no ignition whatsoever during city driving, unless exorbitant amounts of catalyst are employed. To avoid this problem, another energy source is required in the exhaust system to bring either the exhaust gas or the converter itself above the critical temperature required for large χ leading-edge ignition.

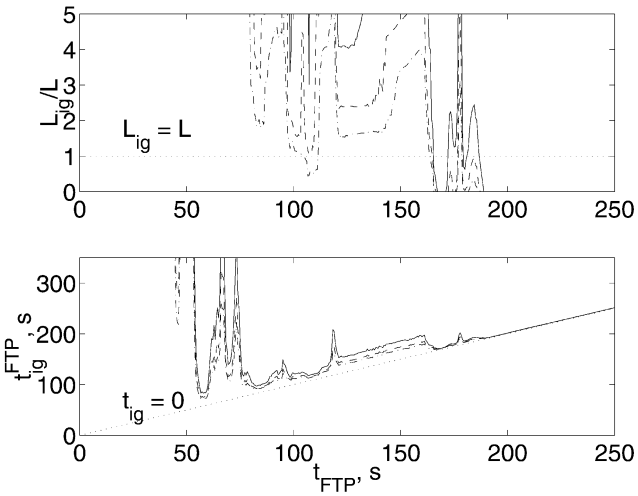

Figure 9. Theoretically computed ignition lengths, L_{ig}, and ignition times, t_{ig}, for the preigniter with different reduced catalyst loading a_{cat}/a_{Oh}, without a hydrocarbon trap.

The solid line is for $a_{cat}/a_{Oh} = 3$, the dashed line is for $a_{cat}/a_{Oh} = 5$, and the dash-dot line is for $a_{cat}/a_{Oh} = 7$. The advantage of increased catalyst loading is clearly seen, as ignition times and lengths are reduced.

Electrically heated preconverter

Electrically heated preconverters (EHCs) are metal preconverters that are attatched to a power supply such as a car battery, and are capable of rapid ignition, as the energy input raises the solid-phase temperature significantly, thus increasing the pollutant reaction rate. This would reduce the amount of catalyst required in the preigniter. Despite these advantages, the technique is considered undesirable to auto manufacturers because, given the conditions in Figure 2, rapid ignition requires over 2,000 W of power. This large power requirement mandates an additional battery, which adds to the vehicle weight and the complexity of the electrical system of the vehicle. Another problem is that high temperatures in the metal may damage the monolith substrates. Either of these scenarios could result in poor pollution conversion efficiency.

In order to utilize the analytical estimate for the ignition of the system subject to the FTP test, an expression must be obtained that predicts the temperature rise inside of the EHC as a result of electric heat. Such an expression can be obtained by integrating Eqs. 3 and 5 to yield steady-state temperature profiles in the absence of reaction. Conduction effects are neglected because the thermal Peclet number is large, as $Pe = U_{\text{eff}} L/\alpha_s = 4{,}300$ when using the thermal velocity in the standard converter, $U_{\text{eff}} = 0.84$ cm/s. The corresponding thermal equations are

$$\epsilon(\rho C_p)_g U \frac{\partial T_g}{\partial x} = hS(T_s - T_g) \tag{30}$$

for the gas and

$$0 = hS(T_g - T_s) + \frac{P}{V_H} \tag{31}$$

for the solid. Using the boundary condition $T_g = T_{\text{in}}$ at $x = 0$ yields

$$T_g = T_{\text{in}} + \frac{x}{\epsilon(\rho C_p)_g U} \frac{P}{V_H} \tag{32}$$

for the gas and

$$T_s = T_{\text{in}} + \frac{P}{V_H}\left(\frac{x}{\epsilon(\rho C_p)_g U} + \frac{1}{hS}\right) \tag{33}$$

for the solid, such that at the reactor exit, when $x = L$,

$$T_s = T_{\text{in}} + \frac{P}{V_H}\left(\frac{L}{\epsilon(\rho C_p)_g U} + \frac{1}{hS}\right). \tag{34}$$

The time for the profiles given by Eqs. 32 and 33 to become valid is simply the convection time for a thermal front to pass through the reactor,

$$t_{\text{conv}} = L\gamma/U, \tag{35}$$

which is less than 3 s for a 2.54-cm metal preconverter using the effective thermal velocity of 0.84 cm/s in the standard monolith. In the previous expressions T_{in} represents the FTP engine-out temperature that is shown in Figure 2. For use in estimating FTP ignition, the mean velocity given by Eq. 26 should be used in estimating the solid-phase temperature given by Eq. 34.

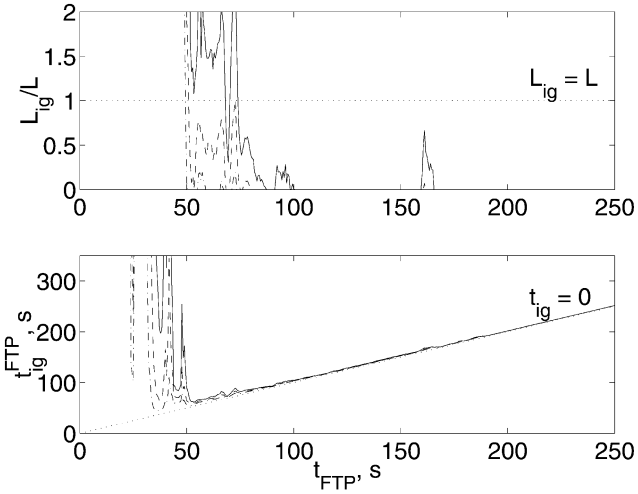

Figure 10. Theoretically computed ignition lengths, L_{ig}, and ignition times, t_{ig}, for the electrically heated catalytic converter with different power inputs.

The solid line is for $P = 1{,}150$ W, the dashed line is for $P = 1{,}500$ W, and the dash-dot line is for $P = 2{,}000$ W. The advantage of increasing power is clearly seen, as ignition times and lengths are dramatically reduced.

Because the solid-phase temperature at $x = L$ is the warmest point in the preconverter, ignition is expected to take place at the reactor exit. Numerical simulations were carried out for EHCs with properties given in Table 1 with various power levels without hydrocarbon traps. As predicted, the ignition in all cases occurs at the exit of the preconverter. However, ignition at this location will occur only when the theoretical ignition length beyond this point is $L_{\text{ig}} = 0$ (large χ, leading-edge ignition). Equation 29 can be used to estimate the time for ignition to take place. Again, results of the analytical model compare well with simulation results. Figure 10 contains a plot of theoretically computed ignition lengths, L_{ig}, and ignition times, t_{ig}, for different power levels. Ignition takes anywhere between 1 and 2 min for these power levels. As a final note, ignition via electrically heated preconverters is undesirable because the ignition always takes place at $x = L$, far downstream of the preconverter entrance. An increase in the gas flow rate will drop the solid temperature at $x = L$, as predicted by Eq. 34. This can extinguish a potential ignition, especially during a lean period.

There have been an increased number of studies in the area of cascaded exhaust systems (Brunson et al., 1993; Socha et al., 1994). Oh et al. (1993) also performed simulations of such a system using the FTP data of Figure 2 with an electric heater upstream of a main catalytic converter. They found that an FTP lightoff occurred in about 75 s, but their converter had a high loading $a_{\text{cat}} = 650$ cm^2 Pt/cm^3 reactor. A converter equipped with the standard loading of $a_{\text{cat}} = 269$

cm^2 Pt/cm^3 reactor would have an increased ignition time. It appears that the ignition seen by Oh et al. (1993) only occurs once the engine-out temperature has plateaued at its maximum during city driving conditions, about 60 s into the FTP and when the mass flow rate is low, as seen in Figure 2. The addition of a light preconverter between the heater and main converter may reduce the ignition time further, but the ignition of the system may still occur via the downstream mechanism in aged systems, and thus is strongly dependent upon the mass flow rate. Waiting for the right moment when the temperature and flow rate are ideal to initiate ignition as this design appears to do is unacceptable, and the current cascaded design fails to meet LEV/ULEV standards and must also be rejected from consideration.

Equation 34 also predicts an increase in the heater exit temperature when the mass flow rate through the heater is decreased. Consequently, if only a fraction of the gas exiting the engine (as little as 10%) flows through the EHC (while the rest of the gas is bypassed to the entrance of the main converter), the temperature of the gas at the heater exit can be high enough to yield a stable, rapid, leading-edge ignition in a preigniter placed immediately downstream of the heater without the need for an additional battery. This is the key concept to a new design, a serial electric heater and preigniter configuration in a judiciously designed bypass stream, that will be discussed in the next section.

Design of an Optimal Converter System

Despite their individual disadvantages, the optimal design will utilize the combination of an electrically heated monolith and a preigniter placed in a bypass stream. The use of a hydrocarbon trap is not vital to the design and is therefore optional. The presence of the bypass stream will also increase the life of these important units by avoiding sintering and poisoning effects in order to provide long-term auto pollution reduction.

The preigniter is chosen because it has a small homogeneous ignition time, t_{ig}^{∞}, due to thin monolith walls and a high catalyst loading. However, there are two key questions associated with the preigniter. The first question relates to noble-metal loading in the preigniter. Can a preigniter be designed with a noble-metal loading much less than 1,344 cm^2 Pt/cm^3 reactor, 5 times the standard loading, that earlier analysis found necessary? The answer lies in the preigniter bypass stream. If flow through the preigniter only occurs during about the first minute and a half to two minutes of a car trip, the noble-metal loading in the preigniter should remain near the fresh value of 1,793 cm^2 Pt/cm^3, since the average car trip is generally around twenty minutes in duration. Therefore, the optimal preigniter can be loaded with the standard loading of any converter, and thus should be inexpensive, as a 2-cm preigniter would only require an additional 20% of precious-metal catalyst beyond the standard converter.

The second question relates to the physical ignition phenomenon in the preigniter: How can the novel converter system be designed in order to achieve a rapid leading-edge ignition in the preigniter? Figure 9 shows that all of the preigniters ignite downstream of the leading edge, a dangerous situation, as the converter can be easily extinguished with an increase in the mass flow rate. The answer to this question lies in the combination of the EHC with the bypass stream, where the flow through the bypass can be adjusted to yield a large temperature rise exiting the preheater. This is because Eq. 32 with $x = L$ shows that a decrease in the velocity in the preheater U leads to a large temperature increase, high enough to lead to a rapid, leading-edge ignition in the preigniter.

In a recent article, Bissett and Oh (1999) found a key parameter $\mu = V_H hS/mC_{p,g}$ that should be of unit order to give the optimum heater performance on pollution reduction. Using the parameters from their earlier analysis (Oh et al., 1993), listed in Table 1, reveals that $\mu = 7.9$ when using the mean flow rate during city driving conditions. In this proposed design, the cross-sectional area of the metal heater is reduced from their standard 89.9 cm^2 to be roughly equal to that of a typical exhaust tailpipe, 20.3 cm^2. In concert, the electric heater length is reduced from the standard 1 in. by a factor of 4 to reduce the transient time required before the gas exiting the converter can reach a prescribed temperature. These design modifications lead to a corresponding reduction of μ to 0.45, more in tune with the optimum predicted by Bissett and Oh's models. Both the bypass and this newly designed EHC will be incorporated into the optimal design. There will be no catalyst placed onto the surface of the EHCs metal substrate. However, catalyst will be incorporated into the short and inexpensive preigniter placed downstream of the electric heater.

Figure 11 shows this newly proposed redesign of the cascaded catalytic converter system, where exhaust gas flows from top to bottom. The system contains thermocouples in four locations. Two thermocouples are placed in the tailpipe at the entrance and exit of the electric heater, which are used to measure the gas temperature rise in the heater. The third thermocouple is placed in the preigniter, about 2.5 mm from its leading edge. This will measure the solid temperature near the entrance of the 2-cm-long preigniter and will inform the system when a leading-edge ignition has taken place. The fourth and final thermocouple in the system will be placed a distance 2 cm from the entrance of the main converter of the standard length, 10 cm. This will inform the system when the main converter is hot enough to sustain an ignition upon the entrance of cold pollution-rich gas.

After the start of an automobile, the newly designed converter system operates in the following manner. The valve in Figure 11 is constantly adjusted via a feedback-control mechanism that diverts a small fraction (around 10–20%) of gas through the left bypass, such that the gas exiting the electric heater is at a set temperature, large enough in magnitude to induce a stable, leading-edge ignition in the preigniter. Its current counterpart, the cascaded exhaust system preigniter, may not ignite at the leading edge or even at all because the feed temperature can fluctuate with sudden starts and stops of the vehicle. For the standard converter, Leighton and Chang (1995) showed that a leading-edge ignition occurs at a feed temperature of 700 K. This was for a poisoned catalyst with loading, $a_{cat} = 269$ cm^2 Pt/cm^3 and a void fraction of $\epsilon = 0.68$. Because the preigniter has a higher void fraction, $\epsilon = 0.88$, and has fresh catalyst, $a_{cat} = 1{,}792$ cm^2 Pt/cm^3, a leading edge ignition can occur at a lower feed temperature. If the bypass system ever fails, however, the catalyst may become poisoned such that the catalyst loading will be reduced,

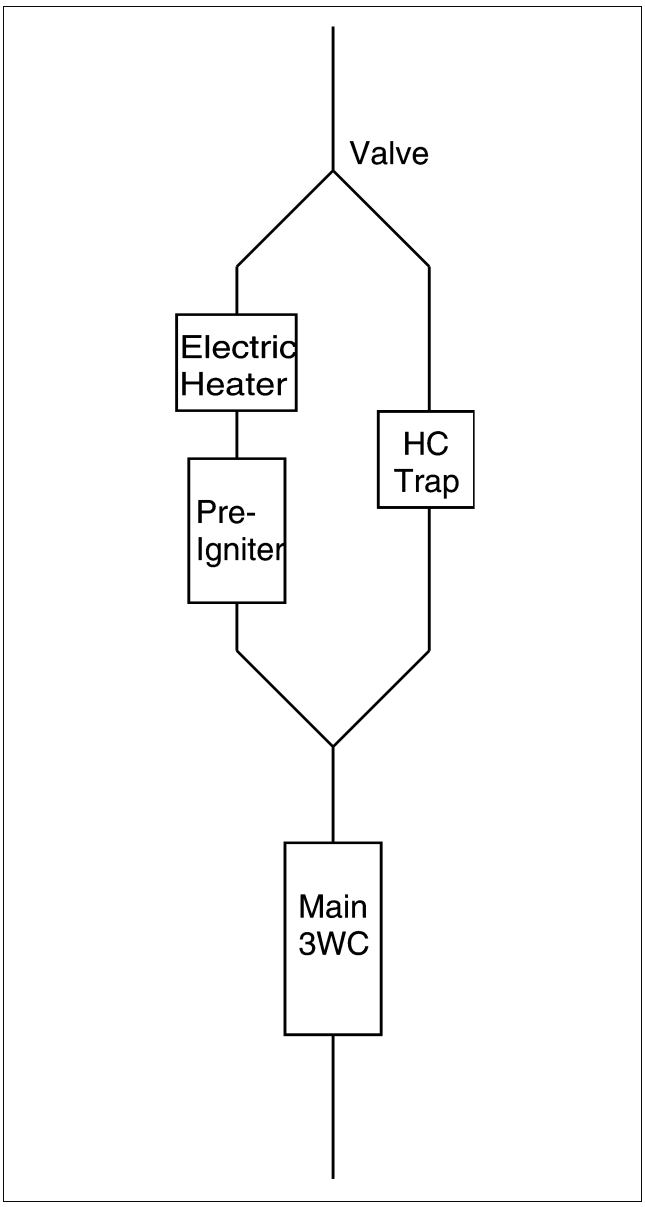

Figure 11. Proposed catalytic converter redesign with an electric heater and preconverter placed in a bypass stream.

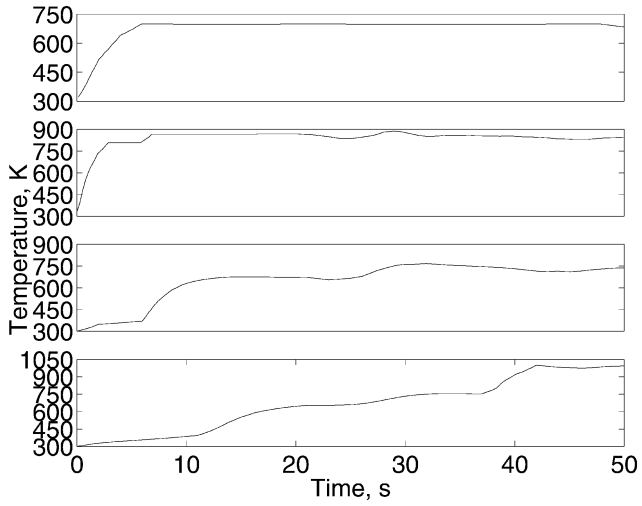

Figure 12. Various simulated temperatures for proposed redesign as a function of time.

(Top graph) Exit gas temperature of preheater. (Second highest graph) Maximum temperature in preigniter. Note that ignition takes place in the preigniter almost instantly. (Third highest graph) Gas temperature exiting the preigniter. At $t = 12$ s the power to the preheater is shut off and all of the engine-out gas is directed through the preigniter, resulting in a rapid temperature rise, as all the pollutant is consumed in the preigniter. (Bottom graph) Maximum temperature in the main converter. At time $t =$ 42 s the bypass stream is removed and the main converter ignites, yielding another rapid temperature rise.

and the ignition may occur downstream at such a temperature. However, leading-edge ignition is ensured for even an aged preigniter if the temperature of the gas leaving the preheater is kept at 700 K. A plot of the gas temperature leaving the preheater as a function of FTP time is shown in Figure 12a, and it can be seen that the exit gas reaches 700 K after 5 s. The engine-out gas temperature, on the other hand, will not reach this value until the vehicle accelerates to highway speeds! The strong advantage of such a design over the standard converter or a preigniter by itself is illustrated in Figure 5.

During this warming up and lightoff process, the majority of the gas exiting the engine proceeds through the channel on the right, until after the thermocouple in the preigniter has sensed ignition. A plot of the maximum temperature in the preigniter, shown in Figure 12b, indicates that the preigniter lights off in about 12 s! At this point, power to the electric heater is cut off and all of the engine-out gas is sent through the preigniter, leading to a large rise in its exit gas temperature, as shown in Figure 12c. This is the temperature of the gas entering the main converter. When the thermocouple in the main converter is at a temperature of about 700 K, only 40 s after the car has been started, as seen in Figure 12d, all of the gas is sent through the right channel, removing the preheater and preigniter from the exhaust system while igniting the main converter at the leading edge. The orientation of the bypass valve will not change any further for the duration of the driving trip.

The power supplied to the metal preheater is chosen to minimize the ignition time in the preconverter without significant heating power consumption, and thus produce minimum pollution emissions at a minimum cost. The lower the power level chosen, the smaller the gas flow rate through the preigniter. Because a reduction in flow rate consequently decreases thermal dispersion in the preigniter, it will increase the time for the thermocouple in the preigniter to detect ignition. An analytical scaling law can be developed to estimate this time for the thermocouple, which is placed an axial distance L_i into the monolith (chosen here to be about 0.25 cm). Simulations indicate that an ignited zone of length L_i at the monolith entrance is unaffected by a strong flow-rate increase upon sudden opening of the bypass valve.

Because the preigniter operates in the large χ limit, thermal dispersion will dominate over convection in heating up the monolith. The time for axial dispersion to heat up the

preigniter an axial distance L_i from the entrance can thus be estimated by

$$t_{\text{diff}} = \frac{L_i^2}{\alpha_{\text{eff}}} = \frac{48}{11}\frac{L_i^2 \alpha_g \gamma}{U_{\text{igniter}}^2 a^2}, \tag{36}$$

where U_{igniter} is the gas velocity in the preigniter, determined from Eq. 32 for the gas temperature exiting the preheater:

$$U_{\text{heater}} = \frac{P}{(T_{\text{out}} - T_{\text{in}})\epsilon(\rho C_p)_g A_H}, \tag{37}$$

where A_H is the cross-sectional area of the preheater. Because the cross-sectional area of the preheater is one-quarter the size of the preigniter, $U_{\text{heater}} = 4U_{\text{igniter}}$. These equations can be combined to give an expression for the diffusion time:

$$t_{\text{diff}} = \frac{768}{11}\frac{L_i^2 \alpha_g \gamma}{P^2}(T_{\text{out}} - T_{\text{in}})^2 \epsilon^2 (\rho C_p)_g^2 A_H^2. \tag{38}$$

In Eq. 38, T_{out} is chosen to be 700 K, because that is the temperature at which both the standard converter and fresh preigniter ignite at the leading edge. T_{in} is taken to be the engine-out temperature, 331 K, immediately after the car has been started. It can be seen in Eq. 38 that reducing the power supply to the heater increases the thermal dispersion time, t_{diff}, because of the reduction in the gas flow rate. This tradeoff yields an optimum power level P, which provides for a stable yet rapid ignition without sacrificing needed energy from the vehicle battery or requiring an additional one.

The time for the exhaust system to reach the operating temperature and be effective in reducing auto pollution is equal to the sum of the preheater convection time, the preigniter ignition time, and the preigniter diffusion time for the thermocouple to sense ignition:

$$t_{\text{eff}} = t_{\text{conv}} + t_{\text{ig}} + t_{\text{diff}}, \tag{39}$$

where t_{conv} is given by Eq. 35, t_{ig} is given by Eq. 24, and t_{diff} is given by Eq. 38. A plot of the theoretical value of t_{eff} as a function of power input to the heater for a value of $L_i = 0.25$ cm is shown in Figure 13. This scaling compares well with simulation results, which are also included in the figure. Since t_{conv} and t_{diff} decay asymptotically to zero with increasing power, a characteristic power value exists, beyond which its sensitivity to power is minimal. The optimum power level is chosen to be this value, roughly at 1,200 W on the bend in the curve. In this case, there will be only 10 s of unabated pollution for a small power supply, a substantial difference when compared with the 170 s in the standard converter! The total energy consumption is 1,200 W $\times$ 10 s = 12.0 kW·s, well within the capacity of the existing 12-V battery in the automobile. The lightoff time may be even less for close-coupled exhaust systems where the engine-out temperatures are higher. In fact, for a given power level P, more of the exhaust gas can be directed through the preheater, leading to a more rapid ignition. At any rate, the prediction of Eq. 39 will still be valid for such circumstances and may even suggest a different optimum power requirement.

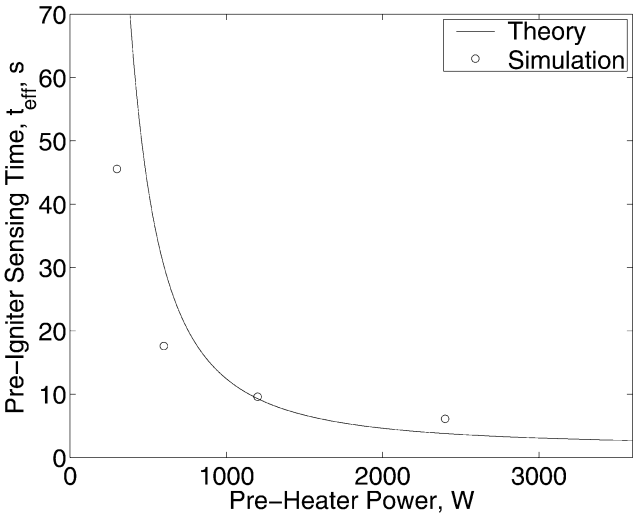

Figure 13. Optimization of power requirement for the catalytic converter redesign.

The theoretical effective ignition time, t_{eff}, is compared with numerical simulations as a function of power supply. The optimum power is chosen to be at the bend in the curve, approximately 1,200 W.

One could also choose to minimize the total energy supplied to the preheater. However, simulation and theory predict that the energy is also insensitive to the power supplied by the battery, provided it is above a critical value of about 1,000 W. This suggests that the optimum should be determined by other means, namely the availability of battery power and the time for the system to ignite (and therefore reduce startup emissions). It would become unnecessary to utilize an additional battery to supply, for instance, 2,400 W of power to the preheater in order to reduce the ignition time to less than 5 s. The optimum system described earlier also allows for the power of the electric heater to be tuned to allow for design errors, catalyst aging, variation in automobiles, and driving conditions.

Conclusions

An optimal catalytic converter system has been described, based on performance under standard conditions and specific federal driving cycles, which will reduce automotive pollution significantly. In addition, the optimal design will ignite at the leading edge of the converter. This type of ignition was shown to be more stable to fluctuations in flow rate than the traditional downstream ignition seen in today's converters, especially during city driving.

The theory presented here is applicable for any federal driving test, as this test varies from automobile to automobile, and for any driving conditions. The controlled exhaust bypass automatically compensates for possible catalyst aging in both the preigniter and the main converter. Other converter systems would require major modification, either by increasing the length or catalyst loading of preigniters or main converters, to be successful. Therefore, the system diagrammed in Figure 11 should be a robust one for improving the lightoff performance of any automobile exhaust system to meet current and future LEV/ULEV requirements.

Acknowledgment

One of the authors (J. M. K.) is supported by a Schmitt fellowship from the University of Notre Dame and by a Bayer fellowship to the Center for Environmental Science and Technology. Another author (H. C. C.) is supported by NSF Grants CTS-9112977 and CTS-9200210.

Notation

a = catalyst pore radius
a_{cat} = catalyst loading
a_{Oh} = standard catalyst loading, 269 cm^2 Pt/cm^3 reactor
A = zeroth-order reaction rate
A_H = heater cross-sectional area
C = pollutant concentration
e = fluctuation amplitude
$f(\chi)$ = ratio of L_{ig}/L_∞
h = heat-transfer coefficient, $h = (24/11)(\kappa_g/a)$
k_m = mass-transfer coefficient
L = bed length
L_{ig} = ignition length
L_∞ = homogeneous ignition length
max = maximum value in specified range
M = mean flow rate
M_g = molecular weight
P = electric power
R = reaction rate
S = monolith pore surface area
T = temperature
t_{conv} = convection time for electric heater
t_{diff} = diffusion time to warm-up preigniter
t_{eff} = effective system lightoff time
t_{ig} = ignition time
t_{ig}^∞ = homogeneous ignition time
U = gas velocity
U_{eff} = thermal velocity, U/γ
V_H = volume of heated element
x = axial position

Greek letters

α_{eff} = thermal dispersivity, $\alpha_{eff} = (11/48)(U^2a^2/\alpha_g\gamma)$
β = inverse Frank-Kamenetskii temperature
γ = heat capacity ratio
ΔH = heat of reaction
ϵ = void fraction
η = degree of monolith subcooling
κ_s = thermal conductivity
μ = Bissett and Oh's dimensionless physical volume ratio (1999)
ρ = density
(ρC_p) = thermal capacitance
τ = fluctuation period
χ = ratio of dispersion to convection

Subscripts and superscripts

FTP = pertaining to FTP driving test
g = gas value
ig = ignition value
o = initial or feed value
s = solid value
∞ = homogeneous value

Literature Cited

Aris, R., "On the Dispersion of a Solute in a Fluid Flowing Through a Tube," *Proc. Roy. Soc. Lond.*, **A235**, 67 (1956).

Bissett, E. J., and S. H. Oh, "Electrically Heated Converters for Automotive Emission Control: Determination of the Best Size Regime for the Heated Element," *Chem. Eng. Sci.*, **54**, 3957 (1999).

Brunson, G., J. E. Kubsh, and W. A. Whittenberger, "Combining Heated and Unheated Core Functions for Improved Cold Start Emissions Performance," SAE Paper 932722, *SAE Trans., Soc. Auto Engr.*, sec. 4, **102**, 1244 (1993).

Burk, P. L., J. K. Hochmuth, D. R. Anderson, S. Sung, A. Punke, U. Dahle, S. J. Tauster, C. O. Tolentino, J. Rogalo, G. Miles, M. Mignano, and M. Niejako, "Cold Start Hydrocarbon Emissions Control Via Admixing Three Way Conversion Catalysts with Heat Exchange and Hydrocarbon Adsorption Phenomena," *Stud. Surf. Sci. Catal.*, **96**, 991 (1995).

Chen, D. K. S., E. J. Bissett, S. H. Oh, and D. L. van Ostrom, "A Three-Dimensional Model for the Analysis of Transient Thermal and Conversion Characteristics of Monolithic Catalytic Converters," SAE Paper 880282, *SAE Trans., Soc. Auto. Engr.*, sec. 4, **97**, 177 (1988).

Jacoby, M, "Getting Auto Exhausts to Pristine," *Chem. Eng. News*, **77**, 36 (Jan. 25, 1999).

Keith, J. M., D. T. Leighton, and H.-C. Chang, "A New High Thermal Dispersion Design for Reverse-Flow Reactors," *Ind. Eng. Chem. Res.*, **38**, 667 (1999).

Kirchner, T., and G. Eigenberger, "Optimization of the Cold-Start Behavior of Automotive Catalysts Using an Electrically Heated Pre-Catalyst," *Chem. Eng. Sci.*, **51**, 2409 (1996).

Lafyatis, D. S., G. P. Ansell, S. C. Bennett, J. C. Frost, P. J. Millington, R. R. Rajaram, A. P. Walker, and T. H. Ballinger, "Ambient Temperature Light-Off for Automobile Emission Control," *Appl. Catal. B: Environ.*, **18**, 123 (1998).

Leighton, D. T., and H.-C. Chang, "A Theory for Fast Igniting Catalytic Converters," *AIChE J.*, **41**, 1898 (1995).

Oh, S. H., and E. J. Bissett, "Mathematical Modeling of Electrically Heated Monolith Converters: Analysis of Design Aspects and Heating Strategy," *Ind. Eng. Chem. Res.*, **33**, 3086 (1994).

Oh, S. H., E. J. Bissett, and P. A. Battiston, "Mathematical Modeling of Electrically Heated Monolith Converters: Model Formulation, Numerical Methods, and Experimental Verification," *Ind. Eng. Chem. Res.*, **32**, 1560 (1993).

Oh, S. H., and J. C. Cavendish, "Transients of Monolithic Catalytic Converters: Response to Step Changes in Feedstream Temperature as Related to Controlling Automobile Emissions," *Ind. Eng. Chem. Prod. Res. Dev.*, **21**, 29 (1982).

Roychoudhurry, S., G. Muench, J. F. Bianchi, W. C. Pfefferle, and F. Gonzales, "Development and Performance of Microlith Light-Off Preconverters for LEV/ULEV," SAE Paper 971023, *SAE Trans., Soc. Auto. Engr.*, sec. 4, **106**, 374 (1997).

Socha, L. S., D. F. Thompson, and P. A. Weber, "Optimization of Extruded Electrically Heated Catalysts," SAE Paper 940468, *SAE Trans., Soc. Auto. Engr.*, sec. 4, **103**, 130 (1994).

Taylor, G. I., "Dispersion of Soluble Matter in Solvent Flowing Slowly Through a Tube," *Proc. Roy. Soc. Lond.*, **A219**, 186 (1953).

Manuscript received May 22, 2000, and revision received Aug. 31, 2000.